

# A numerical investigation on the validity of some recent proposals of inseparability criteria for continuous variable systems: the driven Jaynes-Cummings model

Marcelo A Marchiolli<sup>†</sup>

Instituto de Física de São Carlos, Universidade de São Paulo, Caixa Postal 369, 13560-970 São Carlos, SP, Brazil

E-mail: [marcelo\\_march@bol.com.br](mailto:marcelo_march@bol.com.br)

**Abstract.** Adopting the framework of the Jaynes-Cummings model with an external quantum field, we obtain exact analytical expressions of the normally ordered moments for any kind of cavity and driving fields. Such analytical results are expressed in the integral form, with their integrands having a common term that describes the product of the Glauber-Sudarshan quasiprobability distribution functions for each field, and a kernel responsible for the entanglement. Considering a specific initial state of the tripartite system, the normally ordered moments are then applied to investigate not only the squeezing effect and the nonlocal correlation measure based on the total variance of a pair of Einstein-Podolsky-Rosen type operators for continuous variable systems, but also the Shchukin-Vogel criterion. This kind of numerical investigation constitutes the first quantitative characterization of the entanglement properties for the driven Jaynes-Cummings model.

PACS numbers: 03.65.-w, 03.65.Ud, 03.67.Mn

Submitted to: *J. Phys. A: Math. Gen.*

<sup>†</sup> Correspondence address: Avenida General Osório 414 - centro, 14.870-100 Jaboticabal, SP, Brazil

## 1. Introduction

Entanglement and nonlocal correlations are abstract concepts that naturally appear in quantum mechanics when the superposition principle is applied to composite systems. Nowadays, these concepts play an essential role not only in the quantum computation scenario [1] and quantum information theory [2], but also in the context of relativity theory [3]. For instance, one of the main tasks of quantum information theory (QIT) is to develop a quantitative characterization of the entanglement properties and quantum correlation effects for multipartite physical systems described by continuous and/or discrete variables [4, 5]. In this sense, recent developments in QIT based on the continuous variable regime, with emphasis on quantum optical implementations involving quadrature amplitudes of the electromagnetic field, have appeared in the literature [6-16]. From the theoretical point of view, Duan *et al* [6] have proposed a simple inseparability criterion based on the calculation of the total variance of a pair of Einstein-Podolsky-Rosen (EPR) type operators for continuous variable states. Basically, this criterion states that ‘for any separable continuous variable states, the total variance is bounded from below by a certain value resulting from the uncertainty relation, whereas for entangled states this bound can be exceeded.’ Consequently, the violation of this bound can be interpreted as ‘a sufficient condition for inseparability of the states.’ Pursuing this line, Giedke and co-workers [11] have shown that two-mode squeezed states maximize EPR-like correlations for a fixed amount of entanglement; besides, this result has been used to determine the entanglement of formation for all symmetric gaussian states describing bipartite systems. More recently, Shchukin and Vogel [14] have established an important set of inseparability criteria for bipartite quantum states which is formulated in terms of observable moments associated with a variety of quantum states. To this end, the authors have derived a hierarchy of necessary and sufficient conditions for the negativity of the partial transposition of bipartite quantum states (or sufficient conditions for entanglement) that generalizes some previous purposes from literature.

Now, from the experimental point of view, Josse *et al* [12] have produced in laboratory both quadrature and polarization entanglement via the interaction between a linearly polarized coherent field and a cloud of cold cesium atoms placed in a high finesse optical cavity. To demonstrate continuous variable entanglement in this beautiful experiment, the authors have used the theoretical tools established in [6, 11] – namely, the inseparability criterion and the entanglement of formation – with great success in the experimental data analysis. Furthermore, this experiment has opened new windows of investigation in similar physical systems which describe the matter-field interactions. A feasible physical system to generate continuous variable entanglement is given by the Jaynes-Cummings model (JCM), such theoretical tool being typically realized in cavity-QED experiments involving Rydberg atoms crossing superconducting cavities in different frequency regimes and configurations, with relaxation rates small and well understood [17]. Beyond these fundamental features, it is worth mentioning that multipartite gaussian states have potential applications for quantum teleportation [18, 19] and quantum cryptography [20].

Many authors have investigated the two-mode and driven JCM in different theoretical contexts and predicted new interesting results (for example, see [21-23] and references therein). However, a quantitative characterization of the entanglement properties and a detailed analysis of the nonlocal correlation effects among the constituents (fields and atoms) of these similar physical systems have not frequently

appeared in the literature, and represent two important additional tools in the comprehension of the atom-photon interactions which deserve to be carefully studied. Thus, the main aim of this work is to present the first quantitative characterization of the entanglement properties for the driven JCM, which is based upon the inseparability criteria for continuous variable systems developed in [6, 14]. To this end, we assume the atom is initially prepared in a coherent superposition of ground and excited states, and the cavity and external fields are in the diagonal representation of coherent states. Next, we use the mathematical procedure described in [23] to obtain exact analytical expressions of the normally ordered moments for any kind of cavity and driving fields. These analytical results are then expressed at the integral form with their integrands presenting a common term that describes the product of the Glauber-Sudarshan quasiprobability distribution functions for each field, and a kernel responsible for the nonlocal correlations among the constituents of the tripartite system. To illustrate our results we fix both the cavity and driving fields in a coherent state. In particular, we attain new results within which some of them deserve to be mentioned: (i) we establish a link between squeezing effect and entanglement for different values of detuning frequency in the driven JCM; (ii) we show that EPR uncertainty can not be considered the first quantitative characterization of the entanglement properties of the system under investigation; and finally, (iii) we present a numerical evidence that supports the hierarchy of necessary and sufficient conditions for entanglement derived by Shchukin and Vogel [14].

This work is organized as follows. Section 2 describes the mathematical procedure used in the derivation of exact analytical expressions of the normally ordered moments for the driven JCM. In section 3 we apply our results in the analysis of the squeezing effect for each field fixing, for convenience, both the cavity and driving fields in a coherent state. Moreover, we also analyse (by means of a numerical investigation) the validity of some recent proposals of inseparability criteria for physical systems described by continuous variables (in particular, we consider the EPR uncertainty and the Shchukin-Vogel criterion). Section 4 contains our summary and conclusions. Finally, appendix A shows the main steps to calculate the exact analytical expressions for the generalized moments.

## 2. Derivation of the normally ordered moments

In many textbooks on quantum optics [24], the normally ordered moments are generally defined in terms of an auxiliary function (also denominated as the normal characteristic function) which describes the normal ordering of creation and annihilation operators of the electromagnetic field – i.e.,

$$\Lambda_N(\xi, \xi^*; t) \equiv \text{Tr} [\rho(t) e^{\xi \mathbf{c}^\dagger} e^{-\xi^* \mathbf{c}}] ,$$

$\rho(t)$  being the density operator of the system under investigation. The connection between normally ordered moments and normal characteristic function is promptly established through the relation

$$\langle \mathbf{c}^{\dagger r}(t) \mathbf{c}^s(t) \rangle \equiv \text{Tr} [\rho(t) \mathbf{c}^{\dagger r} \mathbf{c}^s] = (-1)^s \left. \frac{\partial^{r+s}}{\partial \xi^r \partial \xi^{*s}} \Lambda_N(\xi, \xi^*; t) \right|_{\xi, \xi^* = 0}$$

for  $\{r, s\} \in \mathbb{N}$ . However, depending on the circumstances associated with a particular physical system, the connection between normally ordered moments and Wigner

characteristic function is more appropriate to our needs,

$$\langle \mathbf{c}^{\dagger r}(t) \mathbf{c}^s(t) \rangle = (-1)^s \frac{\partial^{r+s}}{\partial \xi^r \partial \xi^{*s}} e^{\frac{1}{2}|\xi|^2} \Lambda_w(\xi, \xi^*; t) \Big|_{\xi, \xi^* = 0}$$

where  $\Lambda_w(\xi, \xi^*; t) \equiv \text{Tr}[\rho(t)\mathbf{D}(\xi)]$  describes the symmetric ordering of the creation and annihilation operators, and  $\mathbf{D}(\xi) = \exp(\xi\mathbf{c}^\dagger - \xi^*\mathbf{c})$  is the displacement operator. Thus, the initial task for both situations consists basically in the calculation of the characteristic functions associated with a physical system of interest described by the density operator  $\rho(t)$ . Consequently, the exact analytical expression of the normally ordered moments will depend on the derivatives of  $\Lambda_N(\xi, \xi^*; t)$  or  $e^{\frac{1}{2}|\xi|^2} \Lambda_w(\xi, \xi^*; t)$  with respect to  $\xi$  and  $\xi^*$  at the point  $\xi, \xi^* = 0$ .

Let us consider the mathematical procedure introduced in [23] to obtain analytical solutions for the atomic inversion and Wigner function in the framework of the driven JCM. In this context, if one assumes the atom is initially prepared in a coherent superposition of ground and excited states, the matrix elements  $\rho_{ij}(t)$  of the tripartite system in the atomic basis are expressed as

$$\begin{aligned} \rho_{11}(t) &= \cos^2(\gamma) \mathbf{U}_{11}(t) \rho_{ab}(0) \mathbf{U}_{11}^\dagger(t) + \frac{1}{2} e^{i\phi} \sin(2\gamma) \mathbf{U}_{11}(t) \rho_{ab}(0) \mathbf{U}_{12}^\dagger(t) \\ &\quad + \frac{1}{2} e^{-i\phi} \sin(2\gamma) \mathbf{U}_{12}(t) \rho_{ab}(0) \mathbf{U}_{11}^\dagger(t) + \sin^2(\gamma) \mathbf{U}_{12}(t) \rho_{ab}(0) \mathbf{U}_{12}^\dagger(t), \\ \rho_{12}(t) &= \cos^2(\gamma) \mathbf{U}_{11}(t) \rho_{ab}(0) \mathbf{U}_{21}^\dagger(t) + \frac{1}{2} e^{i\phi} \sin(2\gamma) \mathbf{U}_{11}(t) \rho_{ab}(0) \mathbf{U}_{22}^\dagger(t) \\ &\quad + \frac{1}{2} e^{-i\phi} \sin(2\gamma) \mathbf{U}_{12}(t) \rho_{ab}(0) \mathbf{U}_{21}^\dagger(t) + \sin^2(\gamma) \mathbf{U}_{12}(t) \rho_{ab}(0) \mathbf{U}_{22}^\dagger(t), \\ \rho_{21}(t) &= \cos^2(\gamma) \mathbf{U}_{21}(t) \rho_{ab}(0) \mathbf{U}_{11}^\dagger(t) + \frac{1}{2} e^{i\phi} \sin(2\gamma) \mathbf{U}_{21}(t) \rho_{ab}(0) \mathbf{U}_{12}^\dagger(t) \\ &\quad + \frac{1}{2} e^{-i\phi} \sin(2\gamma) \mathbf{U}_{22}(t) \rho_{ab}(0) \mathbf{U}_{11}^\dagger(t) + \sin^2(\gamma) \mathbf{U}_{22}(t) \rho_{ab}(0) \mathbf{U}_{12}^\dagger(t), \\ \rho_{22}(t) &= \cos^2(\gamma) \mathbf{U}_{21}(t) \rho_{ab}(0) \mathbf{U}_{21}^\dagger(t) + \frac{1}{2} e^{i\phi} \sin(2\gamma) \mathbf{U}_{21}(t) \rho_{ab}(0) \mathbf{U}_{22}^\dagger(t) \\ &\quad + \frac{1}{2} e^{-i\phi} \sin(2\gamma) \mathbf{U}_{22}(t) \rho_{ab}(0) \mathbf{U}_{21}^\dagger(t) + \sin^2(\gamma) \mathbf{U}_{22}(t) \rho_{ab}(0) \mathbf{U}_{22}^\dagger(t), \end{aligned}$$

where

$$\rho_{ab}(0) = \iint \frac{d^2\alpha_a d^2\alpha_b}{\pi^2} P_a(\alpha_a) P_b(\alpha_b) |\alpha_a, \alpha_b\rangle \langle \alpha_a, \alpha_b|$$

represents the initial density operator for the cavity (*a*) and driving (*b*) fields written in the diagonal representation of coherent states, and  $P(\alpha)$  is the Glauber-Sudarshan quasiprobability distribution function for each field. Furthermore, the matrix elements  $\mathbf{U}_{ij}(t)$  associated with the time-evolution operator are given by

$$\begin{aligned} \mathbf{U}_{11}(t) &= \cos(t\sqrt{\beta_A}) - i \frac{\delta \sin(t\sqrt{\beta_A})}{2\sqrt{\beta_A}}, \\ \mathbf{U}_{12}(t) &= -i\kappa_{\text{eff}} \frac{\sin(t\sqrt{\beta_A})}{\sqrt{\beta_A}} \mathbf{A}, \\ \mathbf{U}_{21}(t) &= -i\kappa_{\text{eff}} \mathbf{A}^\dagger \frac{\sin(t\sqrt{\beta_A})}{\sqrt{\beta_A}}, \\ \mathbf{U}_{22}(t) &= \cos(t\sqrt{\varphi_A}) + i \frac{\delta \sin(t\sqrt{\varphi_A})}{2\sqrt{\varphi_A}}, \end{aligned}$$

with  $\boldsymbol{\varphi}_A = \kappa_{\text{eff}}^2 \mathbf{N}_A + (\delta/2)^2 \mathbf{1}$ ,  $\boldsymbol{\beta}_A = \boldsymbol{\varphi}_A + \kappa_{\text{eff}}^2 \mathbf{1}$ ,  $\mathbf{N}_A = \mathbf{A}^\dagger \mathbf{A}$ ,  $\kappa_{\text{eff}}^2 = \kappa_a^2 + \kappa_b^2$  (effective coupling constant between the atom and an effective field described by the quasi-mode operator  $\mathbf{A}$ ), and  $\delta = \omega_0 - \omega$  (detuning frequency between the atomic transition frequency  $\omega_0$  and the cavity field frequency  $\omega$  – in particular, we assume the resonance condition between the cavity and driving fields). Here,  $\mathbf{A} \equiv \epsilon_a \mathbf{a} + \epsilon_b \mathbf{b}$  is defined by means of annihilation operators  $\mathbf{a}$  (cavity field) and  $\mathbf{b}$  (driving field), with  $\epsilon_{a(b)} = \kappa_{a(b)}/\kappa_{\text{eff}}$  (for more details on the algebraic aspects of this theoretical model, see [23]). Note that  $\boldsymbol{\rho}(t)$  describes the exact solution of the Schrödinger equation in the interaction picture with the nonresonant driven-JCM Hamiltonian. Using this solution we can establish expressions for the time evolution of some quantities (e.g., the Wigner characteristic function and the normally ordered moments for each field) which allow us to shed more light on the nonlocal correlation effects of the atom-photon interaction.

The Wigner characteristic function is expressed into this context in the integral form with their integrands having a common term that describes the product of the Glauber-Sudarshan quasiprobability distribution functions for each field, and a kernel responsible for the nonlocal correlation effects among the constituents of the system under consideration – i.e.,

$$\Lambda_W(\xi, \xi^*; t) = \iint \frac{d^2 \alpha_a d^2 \alpha_b}{\pi^2} P_a(\alpha_a) P_b(\alpha_b) \tilde{K}_{\xi, \xi^*}(\alpha_a, \alpha_b; t) \quad (1)$$

with

$$\begin{aligned} \tilde{K}_{\xi, \xi^*}(\alpha_a, \alpha_b; t) = & \cos^2(\gamma) [{}_{11}D_{\xi, \xi^*}^{11}(\alpha_a, \alpha_b; t) + {}_{21}D_{\xi, \xi^*}^{21}(\alpha_a, \alpha_b; t)] \\ & + \frac{1}{2} e^{i\phi} \sin(2\gamma) [{}_{12}D_{\xi, \xi^*}^{11}(\alpha_a, \alpha_b; t) + {}_{22}D_{\xi, \xi^*}^{21}(\alpha_a, \alpha_b; t)] \\ & + \frac{1}{2} e^{-i\phi} \sin(2\gamma) [{}_{11}D_{\xi, \xi^*}^{12}(\alpha_a, \alpha_b; t) + {}_{21}D_{\xi, \xi^*}^{22}(\alpha_a, \alpha_b; t)] \\ & + \sin^2(\gamma) [{}_{12}D_{\xi, \xi^*}^{12}(\alpha_a, \alpha_b; t) + {}_{22}D_{\xi, \xi^*}^{22}(\alpha_a, \alpha_b; t)] , \end{aligned} \quad (2)$$

and

$${}_{ij}D_{\xi, \xi^*}^{kl}(\alpha_a, \alpha_b; t) = \langle \alpha_a, \alpha_b | \mathbf{U}_{ij}^\dagger(t) \mathbf{D}(\xi) \mathbf{U}_{kl}(t) | \alpha_a, \alpha_b \rangle \quad (3)$$

for  $i, j, k, l = 1, 2$ . Consequently, the next task will consist basically in the calculations of the means values (3) for the cavity and driving fields, and in the derivation of theirs respective normally ordered moments.

## 2.1. Cavity field

The mathematical procedure adopted in the derivation process of the Wigner characteristic function for the cavity (driving) field is based upon the well-established results in the mathematical appendices by Marchiolli and co-workers [23]. Thus, after lengthy calculations, the analytical expressions for the mean values assume the form

$$\begin{aligned} {}_{11}^{(a)}D_{\xi, \xi^*}^{11}(\alpha_a, \alpha_b; t) &= \sum_{\{m, m'\} \in \mathbb{N}} {}_{11}C_{m, m'}^{11}(\alpha_a, \alpha_b) Y_{\xi, \xi^*}^{(m, m')}( \alpha_a, \alpha_b) F_m(t) F_{m'}^*(t) , \\ {}_{21}^{(a)}D_{\xi, \xi^*}^{21}(\alpha_a, \alpha_b; t) &= \sum_{\{m, m'\} \in \mathbb{N}} {}_{21}C_{m+1, m'+1}^{21}(\alpha_a, \alpha_b) Y_{\xi, \xi^*}^{(m+1, m'+1)}( \alpha_a, \alpha_b) \\ &\quad \times \sqrt{(m+1)(m'+1)} G_m(t) G_{m'}^*(t) , \end{aligned}$$

$$\begin{aligned}
{}_{12}^{(a)}D_{\xi, \xi^*}^{11}(\alpha_a, \alpha_b; t) &= \sum_{\{m, m'\} \in \mathbb{N}} {}_{12}C_{m, m'}^{11}(\alpha_a, \alpha_b) Y_{\xi, \xi^*}^{(m, m')}(\alpha_a, \alpha_b) \frac{F_m(t) G_{m'}^*(t)}{\sqrt{m' + 1}}, \\
{}_{22}^{(a)}D_{\xi, \xi^*}^{21}(\alpha_a, \alpha_b; t) &= \sum_{\{m, m'\} \in \mathbb{N}} {}_{22}C_{m+1, m'}^{21}(\alpha_a, \alpha_b) Y_{\xi, \xi^*}^{(m+1, m')}(\alpha_a, \alpha_b) \\
&\quad \times \sqrt{m + 1} G_m(t) F_{m'-1}(t), \\
{}_{11}^{(a)}D_{\xi, \xi^*}^{12}(\alpha_a, \alpha_b; t) &= \sum_{\{m, m'\} \in \mathbb{N}} {}_{11}C_{m, m'}^{12}(\alpha_a, \alpha_b) Y_{\xi, \xi^*}^{(m, m')}(\alpha_a, \alpha_b) \frac{G_m(t) F_{m'}^*(t)}{\sqrt{m + 1}}, \\
{}_{21}^{(a)}D_{\xi, \xi^*}^{22}(\alpha_a, \alpha_b; t) &= \sum_{\{m, m'\} \in \mathbb{N}} {}_{21}C_{m, m'+1}^{22}(\alpha_a, \alpha_b) Y_{\xi, \xi^*}^{(m, m'+1)}(\alpha_a, \alpha_b) \\
&\quad \times \sqrt{m' + 1} F_{m-1}^*(t) G_{m'}^*(t), \\
{}_{12}^{(a)}D_{\xi, \xi^*}^{12}(\alpha_a, \alpha_b; t) &= \sum_{\{m, m'\} \in \mathbb{N}} {}_{12}C_{m, m'}^{12}(\alpha_a, \alpha_b) Y_{\xi, \xi^*}^{(m, m')}(\alpha_a, \alpha_b) \frac{G_m(t) G_{m'}^*(t)}{\sqrt{(m+1)(m'+1)}}, \\
{}_{22}^{(a)}D_{\xi, \xi^*}^{22}(\alpha_a, \alpha_b; t) &= \sum_{\{m, m'\} \in \mathbb{N}} {}_{22}C_{m, m'}^{22}(\alpha_a, \alpha_b) Y_{\xi, \xi^*}^{(m, m')}(\alpha_a, \alpha_b) F_{m-1}^*(t) F_{m'-1}(t),
\end{aligned}$$

where the complex functions  ${}_{ij}C_{m, m'}^{kl}(\alpha_a, \alpha_b)$  and  $Y_{\xi, \xi^*}^{(m, m')}(\alpha_a, \alpha_b)$  are given by

$$\begin{aligned}
{}_{ij}C_{m, m'}^{kl}(\alpha_a, \alpha_b) &= (\epsilon_a \alpha_a + \epsilon_b \alpha_b)^{l-k} [(\epsilon_a \alpha_a + \epsilon_b \alpha_b)^*)^{j-i}] \\
&\quad \times \exp(-|\epsilon_a \alpha_a + \epsilon_b \alpha_b|^2) \frac{|\epsilon_a \alpha_a + \epsilon_b \alpha_b|^{2m}}{m!}
\end{aligned}$$

and

$$\begin{aligned}
Y_{\xi, \xi^*}^{(m, m')}(\alpha_a, \alpha_b) &= \exp\left[-\frac{1}{2}|\xi|^2 + \epsilon_b (\epsilon_b \alpha_a - \epsilon_a \alpha_b)^* \xi - \epsilon_b (\epsilon_b \alpha_a - \epsilon_a \alpha_b) \xi^*\right] \\
&\quad \times [\epsilon_a (\epsilon_a \alpha_a + \epsilon_b \alpha_b)^* \xi]^{m'-m} L_m^{(m'-m)}(\epsilon_a^2 |\xi|^2).
\end{aligned}$$

In these expressions,  $L_n^{(k)}(z)$  denote the associated Laguerre polynomials, and

$$F_m(t) = \cos\left(\frac{\Delta_m t}{2}\right) - i \frac{\delta}{\Delta_m} \sin\left(\frac{\Delta_m t}{2}\right) \quad G_m(t) = -i \frac{\Omega_m}{\Delta_m} \sin\left(\frac{\Delta_m t}{2}\right)$$

correspond to functions responsible for the time evolution of the mean values, with  $\Delta_m^2 = \delta^2 + \Omega_m^2$  and  $\Omega_m = 2\kappa_{\text{eff}}\sqrt{m+1}$  being the effective Rabi frequency. Note that equation (1) can be determined for any states of the cavity and driving fields. For instance, if one considers both the cavity and driving fields in the coherent states, the Wigner characteristic function  $\Lambda_w^{(a)}(\xi, \xi^*; t)$  coincides with  $\tilde{K}_{\xi, \xi^*}^{(a)}(\alpha, \beta; t)$  and consequently, this result generalizes that obtained in [23] for the Wigner function.

Now, let us introduce the auxiliar function

$$\mathfrak{A}_{m, m'}^{(r, s)}(\alpha_a, \alpha_b) = (-1)^s \frac{\partial^{r+s}}{\partial \xi^r \partial \xi^{*s}} e^{\frac{1}{2}|\xi|^2} Y_{\xi, \xi^*}^{(m, m')}(\alpha_a, \alpha_b) \Big|_{\xi, \xi^* = 0} \quad (4)$$

which has the following exact expression:

$$\mathfrak{A}_{m, m'}^{(r, s)}(\alpha_a, \alpha_b) = \begin{cases} \frac{m'!}{m!} \mathfrak{R}_{m, m'}^{(r, s)}(\alpha_a, \alpha_b) \mathfrak{S}_{m, m'}^{(s, r)}(\alpha_a, \alpha_b) & (m' \geq m) \\ \mathfrak{R}_{-m', -m}^{(r, s)}(\alpha_a, \alpha_b) \mathfrak{S}_{m', m}^{(r, s)}(\alpha_a, \alpha_b) \mathfrak{T}^{(m-m')}(\alpha_a, \alpha_b) & (m' \leq m) \end{cases}$$

with

$$\begin{aligned}\mathfrak{R}_{m,m'}^{(r,s)}(\alpha_a, \alpha_b) &= [\epsilon_b (\epsilon_b \alpha_a - \epsilon_a \alpha_b)^*]^r [\epsilon_b (\epsilon_b \alpha_a - \epsilon_a \alpha_b)]^s \left[ \frac{\epsilon_a (\epsilon_a \alpha_a + \epsilon_b \alpha_b)^*}{\epsilon_b (\epsilon_b \alpha_a - \epsilon_a \alpha_b)^*} \right]^{m'-m} \\ \mathfrak{S}_{m,m'}^{(r,s)}(\alpha_a, \alpha_b) &= \sum_{k=0}^{\wp} k! L_k^{(m-k)}(0) L_k^{(r-k)}(0) L_{m'-m+k}^{(s-m'+m-k)}(0) \mathfrak{T}^{(k)}(\alpha_a, \alpha_b) \\ \mathfrak{T}^{(k)}(\alpha_a, \alpha_b) &= \left( \frac{\epsilon_a}{\epsilon_b |\epsilon_b \alpha_a - \epsilon_a \alpha_b|} \right)^{2k}.\end{aligned}$$

Here,  $\wp \equiv \text{Min}[m, r, s - (m' - m)]$  yields the smallest positive integer element of the set  $\{m, r, s - (m' - m)\}$ . One virtue of this auxiliar function is that it allow us to derive an exact analytical expression of the normally ordered moments  $\langle \mathbf{a}^{\dagger r}(t) \mathbf{a}^s(t) \rangle$  for any states of the cavity and driving fields – see the schematic diagram showed below

$$\begin{array}{ccc} Y_{\xi, \xi^*}^{(m, m')}(\alpha_a, \alpha_b) & \longmapsto & \mathfrak{A}_{m, m'}^{(r, s)}(\alpha_a, \alpha_b) \\ \uparrow & & \downarrow \\ {}^{(a)}_{ij} D_{\xi, \xi^*}^{kl}(\alpha_a, \alpha_b; t) & & \langle \mathbf{a}^{\dagger r}(t) \mathbf{a}^s(t) \rangle \\ \uparrow & & \downarrow \\ \tilde{K}_{\xi, \xi^*}^{(a)}(\alpha_a, \alpha_b; t) & \longleftarrow & \Lambda_w^{(a)}(\xi, \xi^*; t) \end{array}$$

where we present the necessary mathematical steps to obtain the normally ordered moments associated with the cavity field. Following, we will establish similar results for the external driving field.

## 2.2. External driving field

Adopting an analogous mathematical procedure for the external driving field, we verify that the mean values  ${}^{(b)}_{ij} D_{\xi, \xi^*}^{kl}(\alpha_a, \alpha_b; t)$  have similar structures to the previous cases but differ in the dependence on the variables  $\xi$  and  $\xi^*$  – i.e., the complex function  $Y_{\xi, \xi^*}^{(m, m')}(\alpha_a, \alpha_b)$  should be adequately replaced by

$$\begin{aligned} Z_{\xi, \xi^*}^{(m, m')}(\alpha_a, \alpha_b) &= \exp \left[ -\frac{1}{2} |\xi|^2 + \epsilon_a (\epsilon_a \alpha_b - \epsilon_b \alpha_a)^* \xi - \epsilon_a (\epsilon_a \alpha_b - \epsilon_b \alpha_a) \xi^* \right] \\ &\quad \times [\epsilon_b (\epsilon_a \alpha_a + \epsilon_b \alpha_b)^* \xi]^{m'-m} L_m^{(m'-m)} (\epsilon_b^2 |\xi|^2)\end{aligned}$$

for each  $i, j, k, l = 1, 2$ . Consequently, the auxiliar function

$$\mathfrak{B}_{m, m'}^{(r, s)}(\alpha_a, \alpha_b) = (-1)^s \frac{\partial^{r+s}}{\partial \xi^r \partial \xi^{s*}} e^{\frac{1}{2} |\xi|^2} Z_{\xi, \xi^*}^{(m, m')}(\alpha_a, \alpha_b) \Big|_{\xi, \xi^* = 0} \quad (5)$$

has a central role in the present approach since its analytical expression

$$\mathfrak{B}_{m, m'}^{(r, s)}(\alpha_a, \alpha_b) = \begin{cases} \frac{m'!}{m!} \mathfrak{Z}_{m, m'}^{(r, s)}(\alpha_a, \alpha_b) \mathfrak{W}_{m, m'}^{(s, r)}(\alpha_a, \alpha_b) & (m' \geq m) \\ \mathfrak{Z}_{-m', -m}^{(r, s)}(\alpha_a, \alpha_b) \mathfrak{W}_{m', m}^{(r, s)}(\alpha_a, \alpha_b) \mathfrak{X}^{(m-m')}(\alpha_a, \alpha_b) & (m' \leq m) \end{cases}$$

with

$$\begin{aligned}\mathfrak{Z}_{m,m'}^{(r,s)}(\alpha_a, \alpha_b) &= [\epsilon_a (\epsilon_a \alpha_b - \epsilon_b \alpha_a)^*]^r [\epsilon_a (\epsilon_a \alpha_b - \epsilon_b \alpha_a)]^s \left[ \frac{\epsilon_b (\epsilon_a \alpha_a + \epsilon_b \alpha_b)^*}{\epsilon_a (\epsilon_a \alpha_b - \epsilon_b \alpha_a)^*} \right]^{m'-m} \\ \mathfrak{W}_{m,m'}^{(r,s)}(\alpha_a, \alpha_b) &= \sum_{k=0}^{\varphi} k! L_k^{(m-k)}(0) L_k^{(r-k)}(0) L_{m'-m+k}^{(s-m'+m-k)}(0) \mathfrak{X}^{(k)}(\alpha_a, \alpha_b) \\ \mathfrak{X}^{(k)}(\alpha_a, \alpha_b) &= \left( \frac{\epsilon_b}{\epsilon_a |\epsilon_a \alpha_b - \epsilon_b \alpha_a|} \right)^{2k}\end{aligned}$$

allows us to derive exact results for  $\langle \mathbf{b}^{\dagger r}(t) \mathbf{b}^s(t) \rangle$  through the Wigner characteristic function  $\Lambda_w^{(b)}(\xi, \xi^*; t)$ . Note that the validity of this auxiliar function obeys the same conditions verified for equation (4). To illustrate our sequence of results, the schematic diagram

$$\begin{array}{ccc} Z_{\xi, \xi^*}^{(m, m')}(\alpha_a, \alpha_b) & \xrightarrow{\hspace{1cm}} & \mathfrak{B}_{m, m'}^{(r, s)}(\alpha_a, \alpha_b) \\ \uparrow & & \downarrow \\ (b) D_{ij}^{kl}(\alpha_a, \alpha_b; t) & & \langle \mathbf{b}^{\dagger r}(t) \mathbf{b}^s(t) \rangle \\ \uparrow & & \downarrow \\ \tilde{K}_{\xi, \xi^*}^{(b)}(\alpha_a, \alpha_b; t) & \xleftarrow{\hspace{1cm}} & \Lambda_w^{(b)}(\xi, \xi^*; t) \end{array}$$

presents the essential steps for obtaining the normally ordered moments associated with the driving field. In the next section we will discuss, in principle, three specific applications for the normally ordered moments with emphasis on the squeezing effect of the electromagnetic fields involved in the driven JCM, the nonlocal correlation measure which is based upon the total variance of a pair of EPR type operators, and the Shchukin-Vogel criterion.

### 3. Applications

Recently, Shchukin and Vogel [14] have further developed the concept of the complete characterization of single-mode nonclassicality (basically, this concept is based on the negativity of the Glauber-Sudarshan quasiprobability distribution function and requires an infinite hierarchy of conditions formulated either in terms of characteristic functions [15] or in terms of observable moments [16]) with the aim of characterising the entanglement of bipartite quantum states for physical systems described by continuous variables. In fact, they have provided necessary and sufficient conditions for the partial transposition of bipartite harmonic quantum states to be nonnegative, such conditions being formulated as an infinite series of inequalities for the moments of the states under investigation. Following the authors, ‘the violation of any inequality of this series is a sufficient condition for entanglement.’ In this section, we will show that the moments derived for the driven JCM not only are considered as a theoretical realization of these conditions but also can be applied, for example, in the study of squeezing effect and in the numerical investigation on the validity of some recent proposals of inseparability criteria.

### 3.1. Squeezing effect

Let us introduce two dimensionless quadrature operators  $\mathbf{Q} = (\mathbf{c}^\dagger + \mathbf{c})/\sqrt{2}$  and  $\mathbf{P} = i(\mathbf{c}^\dagger - \mathbf{c})/\sqrt{2}$  for the electromagnetic field described by the q-number  $\mathbf{c}$ , satisfying the commutation relation  $[\mathbf{Q}, \mathbf{P}] = i\mathbf{1}$ . In general, the squeezing effect occurs when either the variance  $\mathcal{V}_\mathbf{Q}(t) \equiv \langle \mathbf{Q}^2(t) \rangle - \langle \mathbf{Q}(t) \rangle^2$  or  $\mathcal{V}_\mathbf{P}(t) \equiv \langle \mathbf{P}^2(t) \rangle - \langle \mathbf{P}(t) \rangle^2$  assumes values less than  $1/2$  – i.e.,  $\mathcal{V}_\mathbf{Q}(t) < 1/2$  or  $\mathcal{V}_\mathbf{P}(t) < 1/2$ , but not both simultaneously. For convenience in the numerical evaluations the phases  $\gamma$  and  $\phi$ , present in equation (2), will be fixed in  $\gamma = \phi = 0$  throughout this work (this condition is equivalent to assume that the atom was initially prepared in the excited state). Moreover, the initial states of the cavity and driving fields will be also fixed in the coherent states  $\rho_{a(b)}(0) = |\nu_{a(b)}\rangle\langle\nu_{a(b)}|$  (this procedure will diminish considerably the technical difficulties found in the double integrals over the complex  $\alpha_a$ - and  $\alpha_b$ -planes). As a consequence of these assumptions, the normally ordered moments associated with the driven JCM can be written as follow:

$$\begin{aligned} \langle \mathbf{a}^{\dagger r}(t) \mathbf{a}^s(t) \rangle_\ell &= \sum_{m=0}^{\ell} \mathfrak{R}_{m,m}^{(r,s)}(\nu_a, \nu_b) {}_a\Xi_{m,m}^{(r,s)}(\nu_a, \nu_b; t) \\ &+ \sum_{m'=0}^{\ell-1} \sum_{m=m'+1}^{\ell} \mathfrak{R}_{-m', -m}^{(r,s)}(\nu_a, \nu_b) \mathfrak{T}^{(m-m')}(\nu_a, \nu_b) {}_a\Xi_{m,m'}^{(r,s)}(\nu_a, \nu_b; t) \\ &+ \sum_{m=0}^{\ell-1} \sum_{m'=m+1}^{\ell} \mathfrak{R}_{m,m'}^{(r,s)}(\nu_a, \nu_b) {}_a\Phi_{m,m'}^{(s,r)}(\nu_a, \nu_b; t), \end{aligned} \quad (6)$$

$$\begin{aligned} \langle \mathbf{b}^{\dagger r}(t) \mathbf{b}^s(t) \rangle_\ell &= \sum_{m=0}^{\ell} \mathfrak{Z}_{m,m}^{(r,s)}(\nu_a, \nu_b) {}_b\Xi_{m,m}^{(r,s)}(\nu_a, \nu_b; t) \\ &+ \sum_{m'=0}^{\ell-1} \sum_{m=m'+1}^{\ell} \mathfrak{Z}_{-m', -m}^{(r,s)}(\nu_a, \nu_b) \mathfrak{X}^{(m-m')}(\nu_a, \nu_b) {}_b\Xi_{m,m'}^{(r,s)}(\nu_a, \nu_b; t) \\ &+ \sum_{m=0}^{\ell-1} \sum_{m'=m+1}^{\ell} \mathfrak{Z}_{m,m'}^{(r,s)}(\nu_a, \nu_b) {}_b\Phi_{m,m'}^{(s,r)}(\nu_a, \nu_b; t), \end{aligned} \quad (7)$$

where

$$\begin{aligned} {}_a\Xi_{m,m'}^{(r,s)}(\nu_a, \nu_b; t) &= {}_{11}C_{m,m'}^{11}(\nu_a, \nu_b) \mathfrak{S}_{m',m}^{(r,s)}(\nu_a, \nu_b) F_m(t) F_{m'}^*(t) \\ &+ \sqrt{(m+1)(m'+1)} {}_{21}C_{m+1,m'+1}^{21}(\nu_a, \nu_b) \mathfrak{S}_{m'+1,m+1}^{(r,s)}(\nu_a, \nu_b) G_m(t) G_{m'}^*(t) \\ {}_a\Phi_{m,m'}^{(s,r)}(\nu_a, \nu_b; t) &= {}_{11}C_{m,m}^{11}(\nu_a, \nu_b) \mathfrak{S}_{m,m'}^{(s,r)}(\nu_a, \nu_b) F_m(t) F_{m'}^*(t) \\ &+ \sqrt{(m+1)(m'+1)} {}_{21}C_{m+1,m+1}^{21}(\nu_a, \nu_b) \mathfrak{S}_{m+1,m'+1}^{(s,r)}(\nu_a, \nu_b) G_m(t) G_{m'}^*(t) \\ {}_b\Xi_{m,m'}^{(r,s)}(\nu_a, \nu_b; t) &= {}_{11}C_{m,m'}^{11}(\nu_a, \nu_b) \mathfrak{W}_{m',m}^{(r,s)}(\nu_a, \nu_b) F_m(t) F_{m'}^*(t) \\ &+ \sqrt{(m+1)(m'+1)} {}_{21}C_{m+1,m'+1}^{21}(\nu_a, \nu_b) \mathfrak{W}_{m'+1,m+1}^{(r,s)}(\nu_a, \nu_b) G_m(t) G_{m'}^*(t) \\ {}_b\Phi_{m,m'}^{(s,r)}(\nu_a, \nu_b; t) &= {}_{11}C_{m,m}^{11}(\nu_a, \nu_b) \mathfrak{W}_{m,m'}^{(s,r)}(\nu_a, \nu_b) F_m(t) F_{m'}^*(t) \\ &+ \sqrt{(m+1)(m'+1)} {}_{21}C_{m+1,m+1}^{21}(\nu_a, \nu_b) \mathfrak{W}_{m+1,m'+1}^{(s,r)}(\nu_a, \nu_b) G_m(t) G_{m'}^*(t). \end{aligned}$$

Note that the infinite sums present in  ${}_{ij}D_{\xi, \xi^*}^{kl}(\alpha_a, \alpha_b; t)$  were substituted by finite sums,  $\ell$  being the maximum value which guarantees the convergence of these expressions (we have fixed  $\ell = 60$  in the numerical investigations). In fact, exact expressions

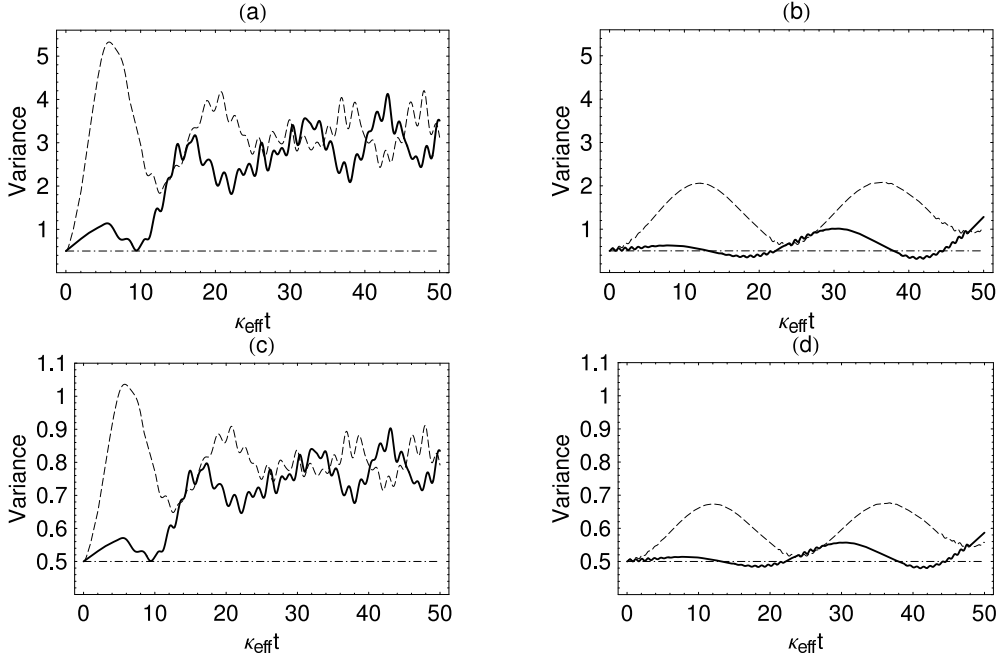


**Figure 1.** Time evolution of variances associated with the quadrature operators  $\mathbf{Q}_{a(b)}(t)$  and  $\mathbf{P}_{a(b)}(t)$  for the cavity (driving) field considering the atom initially prepared in the excited state, and both the cavity and driving fields prepared in the coherent states. Pictures (a) and (b) represent the variances  $V_Q^{(a)}(t)$  (solid line) and  $V_P^{(a)}(t)$  (dashed line) for the following detuning frequencies: (a)  $\delta = 0$  (resonant) and (b)  $\delta = 6\kappa_{\text{eff}}$  (nonresonant), with  $\epsilon_a = 3/\sqrt{10}$ ,  $\epsilon_b = 1/\sqrt{10}$ ,  $|\nu_a| = 1$ , and  $|\nu_b| = 2$  fixed. In addition, pictures (c) and (d) correspond to  $V_Q^{(b)}(t)$  (solid line) and  $V_P^{(b)}(t)$  (dashed line) for the same set of parameters adopted in (a) and (b), respectively. The dot-dashed line present in all pictures refers to the variances of the coherent states (also described in literature as minimum-uncertainty states). Note that the variances show squeezing effect, this effect being directly connected with the amplitude  $|\nu_{a(b)}|$  of the cavity (driving) field and the detuning frequency  $\delta$ .

are reached only in the formal limit  $\ell \rightarrow \infty$ . Such results not only corroborate the mathematical relations established in the schematic diagrams previously showed in section 2, but also lead us to investigate the influence of the detuning on the squeezing effect for the cavity and driving fields separately.

Figure 1 shows the plots of  $V_Q^{(a,b)}(t)$  (solid line) and  $V_P^{(a,b)}(t)$  (dashed line) versus  $\kappa_{\text{eff}} t \in [0, 50]$  when the atom-field system is resonant (a),(c)  $\delta = 0$  and nonresonant (b),(d)  $\delta = 6\kappa_{\text{eff}}$ , for  $\epsilon_a = 3/\sqrt{10}$ ,  $\epsilon_b = 1/\sqrt{10}$ ,  $|\nu_a| = 1$ , and  $|\nu_b| = 2$  fixed. In particular, pictures (a) and (b) represent the variances associated with the quadrature operators  $\mathbf{Q}_a(t)$  and  $\mathbf{P}_a(t)$  (cavity field), while (c) and (d) correspond to the operators  $\mathbf{Q}_b(t)$  and  $\mathbf{P}_b(t)$  (driving field). A superficial analysis of these pictures leads us to conclude that the squeezing effect is linked directly with the amplitude of the cavity (driving) field  $|\nu_{a(b)}|$  and the detuning frequency  $\delta$ . Indeed, numerical investigations for  $|\nu_{a(b)}| \gg 1$  and  $\delta \geq 0$  show that  $V_Q^{(a,b)}(t)$  and  $V_P^{(a,b)}(t)$  have the same asymptotic value  $1/2$ , which minimizes the Heisenberg uncertainty

relation  $\mathcal{V}_{\mathbf{Q}}^{(a,b)}(t)\mathcal{V}_{\mathbf{P}}^{(a,b)}(t) \geq 1/4$ . Furthermore, an interesting aspect of this important effect refers to picture (d), where the variance  $\mathcal{V}_{\mathbf{Q}}^{(b)}(t)$  associated with the single-mode external quantum field exhibits the squeezing effect for  $\delta \neq 0$  (from the experimental point of view, this theoretical prediction can be confirmed through balanced homodyne detections or similar techniques – for instance, see the experimental apparatus used by Josse *et al* [12] in the demonstration of both quadrature and polarization entanglement generated via the interaction between a coherent linearly polarized field and cold atoms in a high finesse optical cavity). Beyond these important points on the squeezing effect, it is worth mentioning that the similarities between the different patterns of curves observed in (a),(c) for  $\delta = 0$  and (b),(d) when  $\delta = 6\kappa_{\text{eff}}$ , can be explained by means of the entanglement dynamics verified in  $\kappa_{\text{eff}}t > 0$  among the constituent parts of the tripartite system (in this case, the continuous variable entanglement for the cavity and driving fields is obtained by tracing over the atomic variables). Thus, for the specific initial states of the cavity and driving fields adopted in this work, we can conclude that squeezing effect and entanglement present an important link in the driven JCM, and this fact leads us to investigate some recent proposals of inseparability criteria for continuous bipartite quantum states. Next, we will focus upon the following question: “Can EPR uncertainty be considered the first quantitative characterization of the entanglement properties of the system under consideration?”

### 3.2. EPR uncertainty

For any bipartite physical system defined in a Hilbert space  $\mathcal{H} = \mathcal{H}_a \otimes \mathcal{H}_b$  and described by an arbitrary normalized density operator  $\rho(t)$ , the total variance of a pair of EPR-like operators – such as  $(\mathbf{Q}_a - \mathbf{Q}_b)/\sqrt{2}$  and  $(\mathbf{P}_a + \mathbf{P}_b)/\sqrt{2}$ , with  $\mathbf{Q}_{a(b)}$  and  $\mathbf{P}_{a(b)}$  satisfying the commutation relation  $[\mathbf{Q}_\alpha, \mathbf{P}_\beta] = i\delta_{\alpha,\beta}\mathbf{1}$  for  $\alpha, \beta = a, b$  – allows us to establish the mathematical relation [6]

$$I_{a,b}(t) = \frac{1}{2} \left[ \mathcal{V}_{\mathbf{Q}}^{(a)}(t) + \mathcal{V}_{\mathbf{Q}}^{(b)}(t) + \mathcal{V}_{\mathbf{P}}^{(a)}(t) + \mathcal{V}_{\mathbf{P}}^{(b)}(t) - 2 \text{Cov}_{\mathbf{Q}}^{(a,b)}(t) + 2 \text{Cov}_{\mathbf{P}}^{(a,b)}(t) \right] \geq 0 \quad (8)$$

where the covariance  $\text{Cov}_{\mathbf{O}}^{(a,b)}(t)$  for the operators  $\mathbf{O}_a \in \mathcal{H}_a$  and  $\mathbf{O}_b \in \mathcal{H}_b$  is given by

$$\text{Cov}_{\mathbf{O}}^{(a,b)}(t) \equiv \frac{1}{2} \text{Tr} [\rho(t)\{\mathbf{O}_a, \mathbf{O}_b\}] - \text{Tr} [\rho(t)\mathbf{O}_a] \text{Tr} [\rho(t)\mathbf{O}_b], \quad (9)$$

and  $\text{Tr} [\rho(t)\{\mathbf{O}_a, \mathbf{O}_b\}]$  represents the anticommutation relation mean value. Note that  $I_{a,b}(t)$  reaches the value zero when  $\rho(t)$  behaves as an idealized EPR type density operator. Furthermore, for states with Gaussian statistics,  $I_{a,b}(t) < 1$  not only implies in the existence of nonlocal correlations but also establishes a sufficient condition for entanglement (in particular, this inseparability criterion has already been used in several experiments to demonstrate continuous variable entanglement – for instance, see [12] and references therein). The additional condition  $I_{a,b}(t) \geq 1$  characterizes separable states into this context. Hence, the quantity  $I_{a,b}(t)$  measures the degree of nonlocal correlations and the inequality (8) defines the EPR uncertainty for  $\rho(t)$ . In appendix A we determine explicitly the generalized moments  $\langle \mathbf{a}^{\dagger p}(t)\mathbf{a}^q(t)\mathbf{b}^{\dagger r}(t)\mathbf{b}^s(t) \rangle$ , which are necessary in the numerical evaluation of the covariance function (9).

Figure 2 shows the plots of  $I_{a,b}(t)$  versus  $\kappa_{\text{eff}}t$  for different values of detuning frequency: (a)  $\delta = 0$ , (b)  $\delta = 6\kappa_{\text{eff}}$ , (c)  $\delta = 20\kappa_{\text{eff}}$ , and (d)  $\delta = 60\kappa_{\text{eff}}$ , where we have adopted the same set of parameters established in the previous figure. Note that EPR uncertainty is completely satisfied in all pictures, but unfortunately it does not

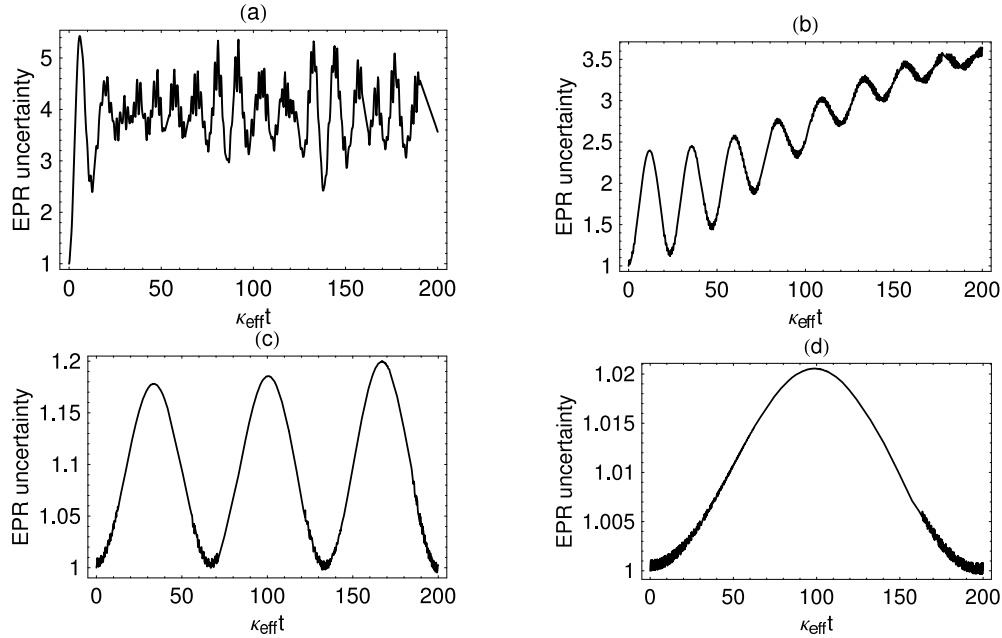


**Figure 2.** Time evolution of  $I_{a,b}(t)$  versus  $\kappa_{\text{eff}}t$  for  $\epsilon_a = 3/\sqrt{10}$ ,  $\epsilon_b = 1/\sqrt{10}$ ,  $|\nu_a| = 1$ , and  $|\nu_b| = 2$  fixed, with different values of detuning frequency: (a)  $\delta = 0$  (resonant regime), (b)  $\delta = 6\kappa_{\text{eff}}$ , (c)  $\delta = 20\kappa_{\text{eff}}$ , and (d)  $\delta = 60\kappa_{\text{eff}}$ . Although the variances associated with the operators  $\mathbf{Q}_a(t)$  and  $\mathbf{Q}_b(t)$  have shown a nonclassical behaviour (squeezing effect) for the nonresonant regime, the EPR uncertainty can not be considered the first quantitative characterization of the entanglement properties in the driven JCM since  $I_{a,b}(t) \geq 1$  for all  $t \geq 0$  (this case characterizes separable states). Beyond this important fact, it is worth mentioning that different initial conditions for the cavity and driving fields can be considered in the study of squeezing and entanglement. However, additional inseparability criteria must be employed in the quantitative characterization of the entanglement properties such as, for example, the Shchukin-Vogel criterion [14].

establish a sufficient condition for entanglement in the driven JCM since  $I_{a,b}(t) \geq 1$ . According to Giedke *et al* [11], the condition  $I_{a,b}(t) < 1$  is met ‘only if at least one of the uncertainties of  $(\mathbf{Q}_a - \mathbf{Q}_b)/\sqrt{2}$  or  $(\mathbf{P}_a + \mathbf{P}_b)/\sqrt{2}$  lies below 1 (the standard quantum limit). This implies that the corresponding states must possess a certain squeezing.’ In this sense, despite  $\mathcal{V}_Q^{(a)}(t)$  and  $\mathcal{V}_Q^{(b)}(t)$  have shown signatures of a nonclassical behaviour (squeezing effect) in pictures 1(b) and 1(d) for  $\delta = 6\kappa_{\text{eff}}$ , the inseparability criterion fails to demonstrate the link between squeezing and entanglement in the theoretical model under study. Similar result was obtained by Shchukin and Vogel [14] for the example of an entangled quantum composed of two coherent states, whose expression reads as

$$|\psi_-\rangle = \left[ 2 \left( 1 - e^{-2(|\alpha|^2 + |\beta|^2)} \right) \right]^{-1/2} (|\alpha, \beta\rangle - |-\alpha, -\beta\rangle).$$

In particular, the authors showed that the inseparability criteria established in [6, 7] fail to demonstrate the entanglement of  $|\psi_-\rangle$ . Consequently, our results lead us to investigate new inseparability criteria based in principle on certain series of inequalities involving higher-order moments which can be applied to a variety of quantum states.

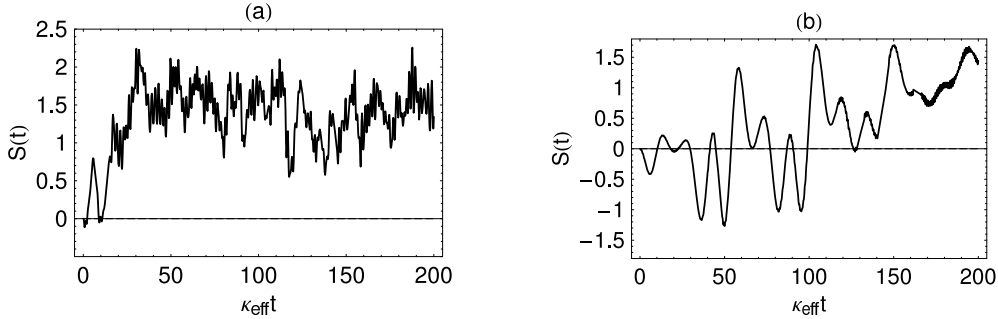


**Figure 3.** Time evolution of  $S(t)$  versus  $\kappa_{\text{eff}}t$  for different values of detuning frequency: (a)  $\delta = 0$  (resonant regime) and (b)  $\delta = 6\kappa_{\text{eff}}$  (nonresonant regime), where we have adopted the same set of parameters established in figure 1. Note that  $S(t)$  assumes negative values in both pictures and this fact corroborates the Shchukin-Vogel criterion for entanglement.

Thus, the next step will consist in the study of simple subdeterminants derived from the Shchukin-Vogel criterion [14] for entanglement.

### 3.3. Shchukin-Vogel criterion

Recently, Shchukin and Vogel [14] derived a hierarchy of necessary and sufficient conditions for the negativity of the partial transposition of bipartite quantum states, which are formulated in terms of observable moments associated with a variety of quantum states. This hierarchy is basically characterized by a set of inseparability criteria (or sufficient conditions for entanglement) that generalizes some previous purposes established in the literature (e.g., see [6-11]). For practical reasons, let us formulate the Shchukin-Vogel criterion as follows:

**Shchukin-Vogel criterion.** The partial transposition of any bipartite quantum state is nonnegative iff all the determinants derived from the  $N$ th order determinant

$$\Gamma_N = \begin{vmatrix} 1 & \langle \mathbf{a} \rangle & \langle \mathbf{a}^\dagger \rangle & \langle \mathbf{b}^\dagger \rangle & \langle \mathbf{b} \rangle & \dots \\ \langle \mathbf{a}^\dagger \rangle & \langle \mathbf{a}^\dagger \mathbf{a} \rangle & \langle \mathbf{a}^{\dagger 2} \rangle & \langle \mathbf{a}^\dagger \mathbf{b}^\dagger \rangle & \langle \mathbf{a}^\dagger \mathbf{b} \rangle & \dots \\ \langle \mathbf{a} \rangle & \langle \mathbf{a}^2 \rangle & \langle \mathbf{a} \mathbf{a}^\dagger \rangle & \langle \mathbf{a} \mathbf{b}^\dagger \rangle & \langle \mathbf{a} \mathbf{b} \rangle & \dots \\ \langle \mathbf{b} \rangle & \langle \mathbf{a} \mathbf{b} \rangle & \langle \mathbf{a}^\dagger \mathbf{b} \rangle & \langle \mathbf{b}^\dagger \mathbf{b} \rangle & \langle \mathbf{a}^2 \rangle & \dots \\ \langle \mathbf{b}^\dagger \rangle & \langle \mathbf{a} \mathbf{b}^\dagger \rangle & \langle \mathbf{a}^\dagger \mathbf{b}^\dagger \rangle & \langle \mathbf{b}^{\dagger 2} \rangle & \langle \mathbf{b} \mathbf{b}^\dagger \rangle & \dots \\ \vdots & \vdots & \vdots & \vdots & \vdots & \dots \end{vmatrix}$$

are nonnegative (in other words,  $\forall N$  we obtain  $\Gamma_N \geq 0$ ). However, if there exists a negative determinant (namely,  $\exists N$  such that  $\Gamma_N < 0$ ) the negativity of the partial transposition has been demonstrated – this fact provides a sufficient condition for any bipartite quantum state under investigation to be entangled.

To illustrate this criterion within the driven JCM we consider, in principle, the time-dependent subdeterminant

$$S(t) = \begin{vmatrix} 1 & \langle \mathbf{b}^\dagger(t) \rangle & \langle \mathbf{a}(t)\mathbf{b}^\dagger(t) \rangle \\ \langle \mathbf{b}(t) \rangle & \langle \mathbf{b}^\dagger(t)\mathbf{b}(t) \rangle & \langle \mathbf{a}(t)\mathbf{b}^\dagger(t)\mathbf{b}(t) \rangle \\ \langle \mathbf{a}^\dagger(t)\mathbf{b}(t) \rangle & \langle \mathbf{a}(t)\mathbf{b}^\dagger(t)\mathbf{b}(t) \rangle & \langle \mathbf{a}^\dagger(t)\mathbf{a}(t)\mathbf{b}^\dagger(t)\mathbf{b}(t) \rangle \end{vmatrix} \quad (10)$$

where the mean values  $\langle \mathbf{a}^{\dagger p}(t)\mathbf{a}^q(t)\mathbf{b}^{\dagger r}(t)\mathbf{b}^s(t) \rangle$  can be evaluated through the results obtained in the appendix A. Figure 3 shows the plots of  $S(t)$  versus  $\kappa_{\text{eff}}t$  for  $\epsilon_a = 3/\sqrt{10}$ ,  $\epsilon_b = 1/\sqrt{10}$ ,  $|\nu_a| = 1$ , and  $|\nu_b| = 2$  fixed, with different values of detuning frequency: (a)  $\delta = 0$  (resonant regime) and (b)  $\delta = 6\kappa_{\text{eff}}$  (nonresonant regime). From these pictures we can observe that  $S(0) = 0$  (this condition refers to separability of the initial density operator for the tripartite system) and when  $\kappa_{\text{eff}}t > 0$ , the time-dependent subdeterminant (10) assumes negative values in both situations (the entanglement condition is promptly verified). In particular, the inseparability of the reduced density operator turns to be more evident in the nonresonant regime – see picture 3(b) – which coincides with the squeezing effect observed in pictures 1(b) and 1(d) for the variances  $\mathcal{V}_{\mathbf{Q}}^{(a)}(t)$  and  $\mathcal{V}_{\mathbf{Q}}^{(b)}(t)$ , respectively. Indeed, the link between squeezing effect and entanglement is established through the detuning frequency  $\delta = \omega_0 - \omega$ , this frequency being associated with the atomic transition ( $\omega_0$ ) and cavity (driving) field ( $\omega$ ) frequencies in the driven JCM. Thus, by means of the numerical evidence obtained in this section, we can conclude that  $S(t)$  corroborates the Shchukin-Vogel criterion and consequently, it can be considered the first quantitative characterization of the entanglement properties for the theoretical model under investigation.

#### 4. Conclusions

In this paper we have applied the decomposition formula for  $\mathfrak{su}(2)$  Lie algebra on the driven Jaynes-Cummings model in order to calculate the exact analytical expressions for the normally ordered moments when the atom is initially prepared in a coherent superposition of ground and excited states. In particular, adopting the diagonal representation of coherent states, we have shown that the Wigner characteristic function can be written in the integral form, with their integrands having a common term which describes the product of the Glauber-Sudarshan quasiprobability distribution functions for each field, and a kernel responsible for the entanglement. Next, we have evaluated the normally ordered moments for the cavity and driving fields separately, by means of their respective Wigner characteristic functions. It is worth emphasizing that the mathematical procedure adopted here does not present any restrictions on the states of the cavity and external electromagnetic fields (for more details, see [23] and references therein). To illustrate our exact results we have fixed, for convenience in the numerical calculations, both the cavity and driving fields in the coherent states. This procedure has allowed us to investigate not only the squeezing effect associated with the quadrature operators  $\mathbf{Q}_{a(b)}(t)$  and  $\mathbf{P}_{a(b)}(t)$  of the cavity (driving) electromagnetic field, but also the validity of the EPR uncertainty and Shchukin-Vogel criterion as inseparability criteria for continuous variable systems. Indeed such numerical investigation has produced important results, within which some deserve to be mentioned: (i) we have shown that squeezing effect and entanglement are directly related to detuning frequency in the driven JCM; (ii) the EPR uncertainty has failed in the description of entanglement properties of the system under consideration; and finally, (iii) we have demonstrated that the Shchukin-Vogel criterion correctly establishes a set of necessary and sufficient conditions for the negativity of partial transposition of bipartite quantum states.

Recently, some outstanding experiments [25-28] have used the concept of entanglement to produce in laboratory certain classes of highly entangled states of multipartite quantum systems. In this sense, we believe that our results can be useful

in the analysis of future experiments or theoretical models in physics involving the generation, manipulation and understanding of this important concept in quantum mechanics.

### Acknowledgments

The author is grateful to Diógenes Galetti and Maurizio Ruzzi from Instituto de Física Teórica (IFT, Unesp, SP, Brazil) for reading the manuscript and for providing valuable suggestions.

### Appendix A. Exact analytical expressions for the generalized moments

The main aim of this appendix is to obtain an exact analytical expression for the generalized moments

$$\langle \mathbf{a}^{\dagger p}(t) \mathbf{a}^q(t) \mathbf{b}^{\dagger r}(t) \mathbf{b}^s(t) \rangle \equiv \text{Tr} [\boldsymbol{\rho}(t) \mathbf{a}^{\dagger p} \mathbf{a}^q \mathbf{b}^{\dagger r} \mathbf{b}^s] \quad (\text{A.1})$$

with  $\{p, q, r, s\} \in \mathbb{N}$ , by means of the Wigner characteristic function

$$\Lambda_w(\xi_a, \xi_a^*, \xi_b, \xi_b^*; t) \equiv \text{Tr} [\boldsymbol{\rho}(t) \mathbf{D}_a(\xi_a) \mathbf{D}_b(\xi_b)] \quad (\text{A.2})$$

which involves the expectation value of the product of displacement operators for each field in the driven JCM. To this end, let us establish the link between both expressions through the mathematical relation [24]

$$\begin{aligned} \langle \mathbf{a}^{\dagger p}(t) \mathbf{a}^q(t) \mathbf{b}^{\dagger r}(t) \mathbf{b}^s(t) \rangle &= (-1)^{q+s} \frac{\partial^{p+q+r+s}}{\partial \xi_a^p \partial \xi_a^{*q} \partial \xi_b^r \partial \xi_b^{*s}} \exp \left[ \frac{1}{2} (|\xi_a|^2 + |\xi_b|^2) \right] \\ &\times \Lambda_w(\xi_a, \xi_a^*, \xi_b, \xi_b^*; t) \Big|_{\xi_a, \xi_a^*, \xi_b, \xi_b^* = 0}. \end{aligned} \quad (\text{A.3})$$

Thus, our first task will consist in obtaining the Wigner characteristic function (A.2), while the second task will focus upon the evaluation of the generalized moments (A.1) with the help of equation (A.3).

Adopting the same mathematical recipe used in section 2 to derive equation (1), the generalized Wigner characteristic function is expressed into this context as

$$\Lambda_w(\xi_a, \xi_a^*, \xi_b, \xi_b^*; t) = \iint \frac{d^2 \alpha_a d^2 \alpha_b}{\pi^2} P_a(\alpha_a) P_b(\alpha_b) \tilde{\mathcal{K}}_{\xi_{a(b)}, \xi_{a(b)}^*}(\alpha_a, \alpha_b; t), \quad (\text{A.4})$$

where  $P_a(\alpha_a)$  and  $P_b(\alpha_b)$  are the Glauber-Sudarshan quasiprobability distribution functions associated with the cavity ( $a$ ) and driving ( $b$ ) fields, and

$$\begin{aligned} \tilde{\mathcal{K}}_{\xi_{a(b)}, \xi_{a(b)}^*}(\alpha_a, \alpha_b; t) &= \cos^2(\gamma) \left[ {}_{11} \mathcal{D}_{\xi_{a(b)}, \xi_{a(b)}^*}^{11}(\alpha_a, \alpha_b; t) + {}_{21} \mathcal{D}_{\xi_{a(b)}, \xi_{a(b)}^*}^{21}(\alpha_a, \alpha_b; t) \right] \\ &+ \frac{1}{2} e^{i\phi} \sin(2\gamma) \left[ {}_{12} \mathcal{D}_{\xi_{a(b)}, \xi_{a(b)}^*}^{11}(\alpha_a, \alpha_b; t) + {}_{22} \mathcal{D}_{\xi_{a(b)}, \xi_{a(b)}^*}^{21}(\alpha_a, \alpha_b; t) \right] \\ &+ \frac{1}{2} e^{-i\phi} \sin(2\gamma) \left[ {}_{11} \mathcal{D}_{\xi_{a(b)}, \xi_{a(b)}^*}^{12}(\alpha_a, \alpha_b; t) + {}_{21} \mathcal{D}_{\xi_{a(b)}, \xi_{a(b)}^*}^{22}(\alpha_a, \alpha_b; t) \right] \\ &+ \sin^2(\gamma) \left[ {}_{12} \mathcal{D}_{\xi_{a(b)}, \xi_{a(b)}^*}^{12}(\alpha_a, \alpha_b; t) + {}_{22} \mathcal{D}_{\xi_{a(b)}, \xi_{a(b)}^*}^{22}(\alpha_a, \alpha_b; t) \right] \end{aligned} \quad (\text{A.5})$$

represents a kernel responsible for the entanglement (or nonlocal correlation effects) between the displacement operators  $\mathbf{D}_a(\xi_a)$  and  $\mathbf{D}_b(\xi_b)$  with

$${}_{ij} \mathcal{D}_{\xi_{a(b)}, \xi_{a(b)}^*}^{kl}(\alpha_a, \alpha_b; t) = \langle \alpha_a, \alpha_b | \mathbf{U}_{ij}^\dagger(t) \mathbf{D}_a(\xi_a) \mathbf{D}_b(\xi_b) \mathbf{U}_{kl}(t) | \alpha_a, \alpha_b \rangle \quad (\text{A.6})$$

for  $i, j, k, l = 1, 2$ . After lengthy calculations, the analytical expressions for the mean values (A.6) assume exact forms similar to that obtained for the cavity field but differ in the dependence on the variables  $\xi_{a(b)}$  and  $\xi_{a(b)}^*$ . As a consequence of this fact, the complex function  $Y_{\xi, \xi^*}^{(m, m')}(\alpha_a, \alpha_b)$  must be adequately substituted by

$$\begin{aligned} \mathcal{H}_{\xi_{a(b)}, \xi_{a(b)}^*}^{(m, m')}(\alpha_a, \alpha_b) = & \exp \left\{ -\frac{1}{2} (|\xi_a|^2 + |\xi_b|^2) + 2i\text{Im} [(\epsilon_b \alpha_a - \epsilon_a \alpha_b)^* (\epsilon_b \xi_a - \epsilon_a \xi_b)] \right\} \\ & \times [(\epsilon_a \alpha_a + \epsilon_b \alpha_b)^* (\epsilon_a \xi_a + \epsilon_b \xi_b)]^{m' - m} L_m^{(m' - m)} (|\epsilon_a \xi_a + \epsilon_b \xi_b|^2) \end{aligned}$$

for each situation described by the indices  $i, j, k, l = 1, 2$ . In particular, if one considers the initial states of the cavity and driving fields in the coherent states (for instance,  $\rho_{a(b)}(0) = |\nu_{a(b)}\rangle\langle\nu_{a(b)}|$ ), we obtain  $\Lambda_w(\xi_a, \xi_a^*, \xi_b, \xi_b^*; t) = \tilde{\mathcal{K}}_{\xi_{a(b)}, \xi_{a(b)}^*}(\nu_a, \nu_b; t)$  and for  $\gamma = \phi = 0$  fixed, this characteristic function assumes the simple form

$$\Lambda_w(\xi_a, \xi_a^*, \xi_b, \xi_b^*; t) = {}_{11}\mathcal{D}_{\xi_{a(b)}, \xi_{a(b)}^*}^{11}(\nu_a, \nu_b; t) + {}_{21}\mathcal{D}_{\xi_{a(b)}, \xi_{a(b)}^*}^{21}(\nu_a, \nu_b; t). \quad (\text{A.7})$$

Following, we will use (A.4) to derive an exact analytical expression for the generalized moments (A.3).

Let us initially introduce the generating function for  $\mathcal{H}_{\xi_{a(b)}, \xi_{a(b)}^*}^{(m, m')}(\alpha_a, \alpha_b)$  through the definition

$$\mathcal{H}_{\xi_{a(b)}, \xi_{a(b)}^*}^{(m, m')}(\alpha_a, \alpha_b) = \frac{1}{m!} \frac{\partial^{m+m'}}{\partial u^m \partial v^{m'}} \mathcal{G}_{\xi_{a(b)}, \xi_{a(b)}^*}^{(u, v)}(\alpha_a, \alpha_b) \Big|_{u, v=0} \quad (\text{A.8})$$

where

$$\mathcal{G}_{\xi_{a(b)}, \xi_{a(b)}^*}^{(u, v)}(\alpha_a, \alpha_b) = \sum_{\{k, k'\} \in \mathbb{N}} \mathcal{H}_{\xi_{a(b)}, \xi_{a(b)}^*}^{(k, k')}(\alpha_a, \alpha_b) \frac{u^k v^{k'}}{k'!}. \quad (\text{A.9})$$

Furthermore, we also consider the auxiliar function

$$\begin{aligned} \mathcal{I}_{m, m'}^{(p, q, r, s)}(\alpha_a, \alpha_b) = & (-1)^{q+s} \frac{\partial^{p+q+r+s}}{\partial \xi_a^p \partial \xi_a^{*q} \partial \xi_b^r \partial \xi_b^{*s}} \exp \left[ \frac{1}{2} (|\xi_a|^2 + |\xi_b|^2) \right] \\ & \times \mathcal{H}_{\xi_{a(b)}, \xi_{a(b)}^*}^{(m, m')}(\alpha_a, \alpha_b) \Big|_{\xi_a, \xi_a^*, \xi_b, \xi_b^* = 0} \end{aligned} \quad (\text{A.10})$$

which has a fundamental role in the present context since this function should reduce the complexity of our calculations. Indeed, substituting (A.8) into equation (A.10) we obtain promptly the following useful relation:

$$\mathcal{I}_{m, m'}^{(p, q, r, s)}(\alpha_a, \alpha_b) = \frac{1}{m!} \frac{\partial^{m+m'}}{\partial u^m \partial v^{m'}} \mathcal{J}_{u, v}^{(p, q, r, s)}(\alpha_a, \alpha_b) \Big|_{u, v=0} \quad (\text{A.11})$$

with  $\mathcal{J}_{u, v}^{(p, q, r, s)}(\alpha_a, \alpha_b)$  given by

$$\begin{aligned} \mathcal{J}_{u, v}^{(p, q, r, s)}(\alpha_a, \alpha_b) = & (-1)^{q+s} \frac{\partial^{p+q+r+s}}{\partial \xi_a^p \partial \xi_a^{*q} \partial \xi_b^r \partial \xi_b^{*s}} \exp \left[ \frac{1}{2} (|\xi_a|^2 + |\xi_b|^2) \right] \\ & \times \mathcal{G}_{\xi_{a(b)}, \xi_{a(b)}^*}^{(u, v)}(\alpha_a, \alpha_b) \Big|_{\xi_a, \xi_a^*, \xi_b, \xi_b^* = 0}. \end{aligned} \quad (\text{A.12})$$

For instance, the generating function (A.9) reads as

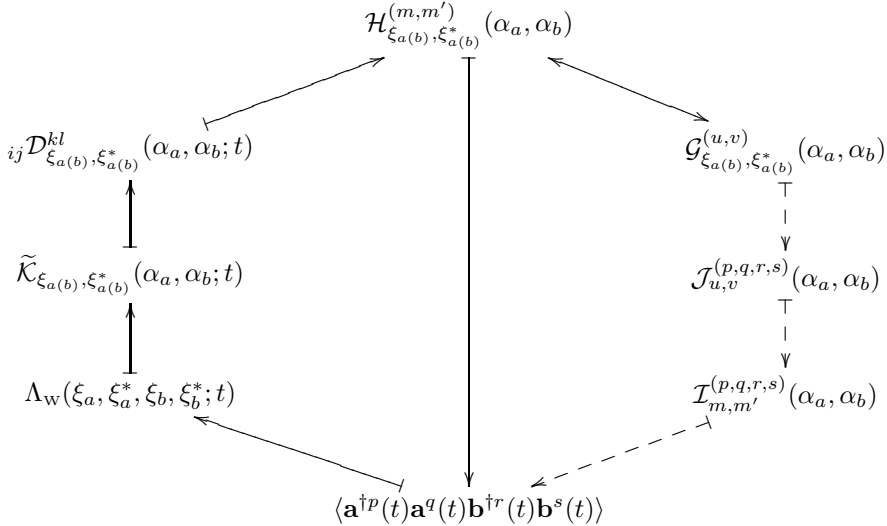
$$\begin{aligned} \mathcal{G}_{\xi_{a(b)}, \xi_{a(b)}^*}^{(u,v)}(\alpha_a, \alpha_b) = & \exp \left\{ -\frac{1}{2} (|\xi_a|^2 + |\xi_b|^2) + 2i\text{Im} [(\epsilon_b \alpha_a - \epsilon_a \alpha_b)^* (\epsilon_b \xi_a - \epsilon_a \xi_b)] \right\} \\ & \times \exp \left[ -\frac{(\epsilon_a \xi_a + \epsilon_b \xi_b)^*}{(\epsilon_a \alpha_a + \epsilon_b \alpha_b)^*} u + (\epsilon_a \alpha_a + \epsilon_b \alpha_b)^* (\epsilon_a \xi_a + \epsilon_b \xi_b) v + uv \right] \end{aligned}$$

while (A.12) has the explicit expression

$$\begin{aligned} \mathcal{J}_{u,v}^{(p,q,r,s)}(\alpha_a, \alpha_b) = & [\epsilon_a (\epsilon_a \alpha_a + \epsilon_b \alpha_b)^* v + \epsilon_b (\epsilon_b \alpha_a - \epsilon_a \alpha_b)^*]^p \\ & \times \left[ \frac{\epsilon_a u}{(\epsilon_a \alpha_a + \epsilon_b \alpha_b)^*} + \epsilon_b (\epsilon_b \alpha_a - \epsilon_a \alpha_b) \right]^q \\ & \times [\epsilon_b (\epsilon_a \alpha_a + \epsilon_b \alpha_b)^* v - \epsilon_a (\epsilon_b \alpha_a - \epsilon_a \alpha_b)^*]^r \\ & \times \left[ \frac{\epsilon_b u}{(\epsilon_a \alpha_a + \epsilon_b \alpha_b)^*} - \epsilon_a (\epsilon_b \alpha_a - \epsilon_a \alpha_b) \right]^s \exp(uv). \end{aligned}$$

Consequently, the partial derivatives of this expression with respect to  $u$  and  $v$  at the point  $u, v = 0$  allow us to determine the auxiliar function (A.11).

Finally, it is worth mentioning that the generalized moments for any kind of cavity and driving fields can be obtained by means of a basic sequence of functions evaluated in this appendix – e.g., the schematic diagram showed below



represents two alternative ways of finding out the generalized moments (A.1). From the theoretical point of view, (A.1) plays an essential role not only in the investigation process of the squeezing effect and EPR uncertainty, but also in the analysis of the Shchukin-Vogel criterion for entanglement in the driven JCM.

## References

- [1] Galindo A and Martin-Delgado M A 2002 Information and computation: Classical and quantum aspects *Rev. Mod. Phys.* **74** 347
- [2] Keyl M 2002 Fundamentals of quantum information theory *Phys. Rep.* **369** 431
- [3] Peres A and Terno D R 2004 Quantum information and relativity theory *Rev. Mod. Phys.* **76** 93

- [4] Braunstein S L and van Loock P 2005 Quantum information with continuous variables *Rev. Mod. Phys.* **77** 513
- [5] Mintert F, Carvalho A R R, Kuš M and Buchleitner A 2005 Measures and dynamics of entangled states *Phys. Rep.* **415** 207
- [6] Duan L-M, Giedke G, Cirac J I and Zoller P 2000 Inseparability Criterion for Continuous Variable Systems *Phys. Rev. Lett.* **84** 2722
- [7] Simon R 2000 Peres-Horodecki Separability Criterion for Continuous Variable Systems *Phys. Rev. Lett.* **84** 2726
- [8] Werner R F and Wolf M M 2001 Bound Entangled Gaussian States *Phys. Rev. Lett.* **86** 3658
- [9] Giedke G, Kraus B, Lewenstein M and Cirac J I 2001 Entanglement Criteria for All Bipartite Gaussian States *Phys. Rev. Lett.* **87** 167904
- [10] Giedke G, Duan L-M, Cirac J I and Zoller P 2002 Distillability criterion for all bipartite gaussian states *Quantum Inf. Comput.* **1** 79
- [11] Giedke G, Wolf M M, Krüger O, Werner R F and Cirac J I 2003 Entanglement of Formation for Symmetric Gaussian States *Phys. Rev. Lett.* **91** 107901
- [12] Josse V, Dantan A, Bramati A, Pinardi M and Giacobino E 2004 Continuous Variable Entanglement using Cold Atoms *Phys. Rev. Lett.* **92** 123601
- [13] Kheruntsyan K V, Olsen M K and Drummond P D 2005 Einstein-Podolsky-Rosen Correlations via Dissociation of a Molecular Bose-Einstein Condensate *Phys. Rev. Lett.* **95** 150405
- [14] Shchukin E and Vogel W 2005 Inseparability criteria for continuous bipartite quantum states *Phys. Rev. Lett.* **95** 230502
- [15] Richter Th and Vogel W 2002 Nonclassicality of Quantum States: A Hierarchy of Observable Conditions *Phys. Rev. Lett.* **89** 283601
- [16] Shchukin E, Richter Th and Vogel W 2005 Nonclassicality criteria in terms of moments *Phys. Rev. A* **71** 011802(R); Shchukin E V and Vogel W 2005 Nonclassical moments and their measurement *Phys. Rev. A* **72** 043808
- [17] Raimond J M, Brune M and Haroche S 2001 *Colloquium: manipulating quantum entanglement with atoms and photons in a cavity* *Rev. Mod. Phys.* **73** 565 and references therein
- [18] Furusawa A, Sørensen J L, Braunstein S L, Fuchs C A, Kimble H J and Polzik E S 1998 Unconditional Quantum Teleportation *Science* **282** 706
- [19] Adesso G and Illuminati F 2005 Equivalence between Entanglement and the Optimal Fidelity of Continuous Variable Teleportation *Phys. Rev. Lett.* **95** 150503
- [20] Grosshans F, Assche G V, Wenger J, Brouri R, Cerf N J and Grangier P 2003 Quantum key distribution using gaussian-modulated coherent states *Nature (London)* **421** 238
- [21] Solano E, Agarwal G S and Walther H 2003 Strong-driving-assisted multipartite entanglement in cavity QED *Phys. Rev. Lett.* **90** 027903
- [22] Wildfeuer C and Schiller D H 2003 Generation of entangled  $N$ -photon states in a two-mode Jaynes-Cummings model *Phys. Rev. A* **67** 053801
- [23] Marchiolli M A, Missori R J and Roversi J A 2003 Qualitative aspects of entanglement in the Jaynes-Cummings model with an external quantum field *J. Phys. A: Math. Gen.* **36** 12275
- [24] For example, see the following textbooks: Louisell W H 1973 *Quantum Statistical Properties of Radiation* (New York: John Wiley); Nussenzveig H M 1973 *Introduction to Quantum Optics* (New York: Gordon and Breach Science Publishers); Barnett S M and Radmore P M 1997 *Methods in Theoretical Quantum Optics* (New York: Oxford University Press); Scully M O and Zubairy M S 1997 *Quantum Optics* (New York: Cambridge University Press); Orszag M 2000 *Quantum Optics* (Berlin: Springer)
- [25] Leibfried D, Knill E, Seidelin S, Britton J, Blakestad R B, Chiaverini J, Hume D B, Itano W M, Jost J D, Langer C, Ozeri R, Reichle R and Wineland D J 2005 Creation of a six-atom ‘Schrödinger cat’ state *Nature (London)* **438** 639
- [26] Häffner H, Hänsel W, Roos C F, Benhelm J, Chek-al-kar D, Chwalla M, Körber T, Rapol U D, Riebe M, Schmidt P O, Becher C, Gühne O, Dür W and Blatt R 2005 Scalable multiparticle entanglement of trapped ions *Nature (London)* **438** 643
- [27] Chou C W, de Riedmatten H, Felinto D, Polyakov S V, van Enk S J and Kimble H J 2005 Measurement-induced entanglement for excitation stored in remote atomic ensembles *Nature (London)* **438** 828
- [28] Chanelière T, Matsukevich D N, Jenkins S D, Lan S -Y, Kennedy T A B and Kuzmich A 2005 Storage and retrieval of single photons transmitted between remote quantum memories *Nature (London)* **438** 833